

Supporting information:
pH-dependent solution dynamics of a manganese(II)
polyoxometalate, $[\text{Mn}_4(\text{H}_2\text{O})_2(\text{P}_2\text{W}_{15}\text{O}_{56})_2]^{16-}$, and $[\text{Mn}(\text{H}_2\text{O})_6]^{2+}$.

Rupali Sharma¹, Jie Zhang¹, and C. André Ohlin¹

¹School of Chemistry, Monash University, Victoria, Australia

Contents

1	Synthesis and characterisation of $\text{Na}_{15}\text{H}[\text{Mn}_4(\text{H}_2\text{O})_2(\text{P}_2\text{W}_{15}\text{O}_{56})_2] \cdot 70 \text{H}_2\text{O}$ (1)	3
2	Determination of pH stability	3
2.1	Potentiometric titration	3
2.2	UV/VIS titration	5
3	^{17}O NMR spectroscopy	5
3.1	Data acquisition	5
3.2	Data processing	6
3.3	Calculation of rate using difference in line-width with and without paramagnetic ion	9
3.4	Error propagation	10

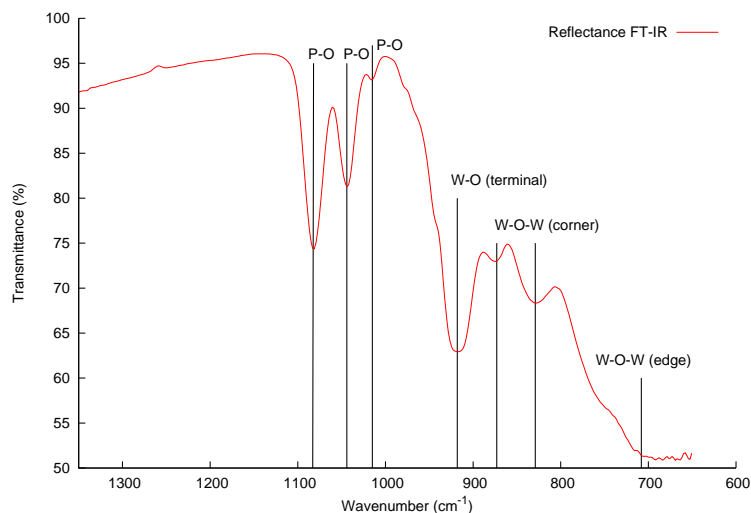


Figure S1: ATR FT-IR spectrum of $\text{Na}_{15}\text{H}[\text{Mn}_4(\text{H}_2\text{O})_2(\text{P}_2\text{W}_{15}\text{O}_{56})_2]\cdot 70\text{H}_2\text{O}$. The spectrum was acquired on a Cary 640 FT-IR instrument.

1 Synthesis and characterisation of $\text{Na}_{15}\text{H}[\text{Mn}_4(\text{H}_2\text{O})_2(\text{P}_2\text{W}_{15}\text{O}_{56})_2]\cdot 70\text{H}_2\text{O}$ (**1**)

$\text{Na}_{12}[\alpha\text{-P}_2\text{W}_{15}\text{O}_{56}]\cdot 24\text{H}_2\text{O}$ was synthesised according to literature.[1] $\alpha\beta\beta\alpha\text{-Na}_{15}\text{H}[\text{Mn}_4(\text{H}_2\text{O})_2(\text{P}_2\text{W}_{15}\text{O}_{56})_2]\cdot 70\text{H}_2\text{O}$ (**1**) was synthesised according to a published procedure.[2] Briefly, $\text{Mn}(\text{NO}_3)_2 \cdot 4\text{H}_2\text{O}$ (2.5 mmol, 0.63 g) was dissolved in $\text{NaCl}(\text{aq})$ (1 M, 50 ml). $\text{Na}_{12}\text{P}_2\text{W}_{15}\text{O}_{56}$ (1 mmol, 4 g) was added very slowly, and the mixture heated at 60°C until a transparent solution was obtained. The solution was warm filtered through paper to remove any insoluble solids and then left at room temperature to crystallise. The crystals obtained were isolated, washed repeatedly with cold $\text{NaCl}(\text{aq})$ (2 M) solution on a medium frit with suction, until the filtrate was colourless. The compound was dried in a desiccator at room temperature.

Elemental analyses were carried out by Galbraith Laboratories, Inc. (Knoxville, TN). Elemental analysis calculated (found) for **1**: Na 3.76 (3.72), P 1.26 (1.33), Mn 2.33 (2.37), W 59.1 (59.5) %w/w.

Thermogravimetric analysis, performed on a Mettler Toledo TGA TSC 1, indicated 70 crystal waters per cluster molecule. The ATR FT-IR (fig. 1) agreed with the literature.[2]

A cyclic voltammogram was recorded of an N_2 purged solution of **1** (0.97 mM) at pH 4.0 (0.1 M CH_3COONa , 0.1 M CH_3COOH ; 0.05 M Na_2SO_4) using a three-electrode set up (Ag/AgCl in 3 M NaCl reference; glassy carbon working electrode; Pt wire counter electrode) with a scan rate of 20 mV s^{-1} (see figure S2). The obtained voltammogram agrees with literature.[3] There is no evidence of irreversible waves which would indicate free $[\text{Mn}(\text{H}_2\text{O})_6]^{2+}$.

^{31}P NMR spectra were acquired on a Bruker DPX 300 (7.05 T, ^{31}P 121.49 MHz) spectrometer equipped with a 5 mm broadband probe. The ^{31}P chemical shifts were measured at 298 K and calibrated against an external H_3PO_4 (85 %) reference.

2 Determination of pH stability

2.1 Potentiometric titration

A sample **1** (3.89 mM, 5 ml, 0.1 M NaClO_4) was titrated on a Metrohm 736 GP Titrino from the self-buffering pH (6.82) to pH 2.97 using HClO_4 (111 mM, 0.1 M NaClO_4). The burette was then changed to

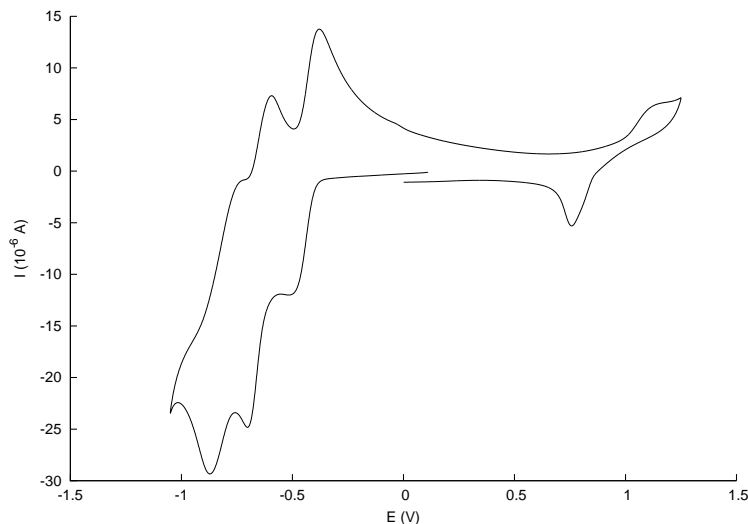


Figure S2: Cyclic voltammogram of **1**. W(IV)/W(V) waves on the left and Mn(II)/Mn(III) waves on the right. Initial scan direction left. See section 1 in text for details.

NaOH (101 mM, 0.1 M NaClO₄) and the sample was titrated back to pH 8.29.

The amount of uncompensated excess charge per mol of **1**, z_e , was plotted as a function of pH. The z_e value can be calculated from the complete mass-charge balance of the titrated NaClO₄/HClO₄ system.[4] Briefly, for a pH active, multiply charged species (Mⁿ⁻), the total concentration of M, M_{tot} is the sum of M in all the possible protonation states (eq. S1). z_{tot} is the sum of all the charges in the system (eq. S3), and should be exactly zero if all charges are accounted for. For a multiprotic acid where the pK_as are unknown, z_M , the sum of all the charge contributed by M in its different protonation states, is unknown (eq. S3). As $z_{tot} \equiv 0$, by defining $z_e = \frac{z_M}{[M_{tot}]}$, we can calculate the **variation** in the excess uncompensated charge per molecule (eq. S4). We can thus see protonation events, although the exact protonation state may not be known.

$$M_{tot} = [M^{n-}] + [HM^{(n-1)}] + [H_2M^{(n-2)}] + \dots \quad (S1)$$

$$z_{tot} = [Na^+] + [H^+] - [OH^-] - [ClO_4^-] + (-n) \cdot [M^{n-}] + (-(n-1)) \cdot [M^{-(n-1)}] + \dots \quad (S2)$$

$$= [Na^+] + [H^+] - [OH^-] - [ClO_4^-] + z_M \quad (S3)$$

$$z_e = - \frac{[Na^+] + [H^+] - [OH^-] - [ClO_4^-]}{[M_{tot}]} \quad (S4)$$

The stable pH region for **1** was defined as the region where the z_e curves overlapped, which was pH 3-7 (fig. 2A). A pK_a, 4.4±0.0(2), was determined by fitting the z_e values to equation S10 (see eq. S5-S9 for derivation).

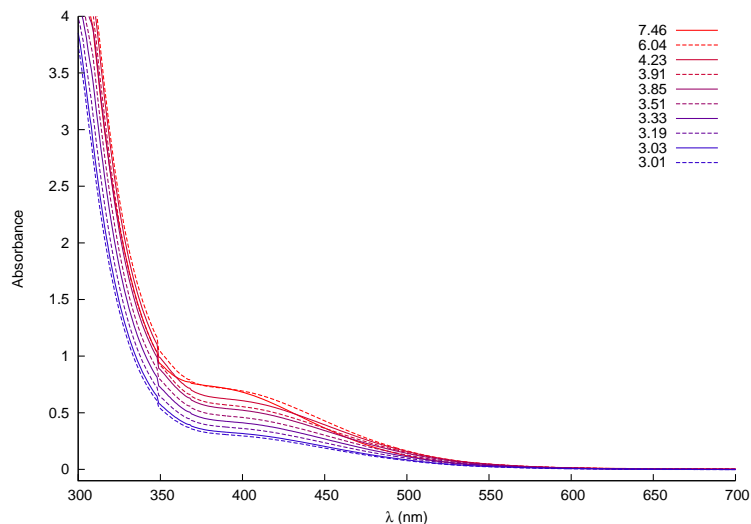


Figure S3: Successive absorption spectra of **1** as a function of pH. Absorbance decreases as pH shifts from basic to acidic conditions (Blue – more acidic. Red – more alkaline).

$$K_a = \frac{[\text{H}][\text{A}]}{[\text{HA}]} \quad (\text{S5})$$

$$K_a = \frac{[\text{H}][x_A]}{1 - x_A} \Leftrightarrow \quad (\text{S6})$$

$$x_A = \frac{K_a}{[\text{H}] + K_a} \quad (\text{S7})$$

$$x_A = \frac{10^{-pK_a}}{10^{-pH} + 10^{-pK_a}} \quad (\text{S8})$$

$$z_e = (1 - x_A)z_{HA} + x_A z_A \quad (\text{S9})$$

$$z_{HA} = 0$$

$$z_e = z_A \frac{10^{-pK_a}}{10^{-pH} + 10^{-pK_a}} \quad (\text{S10})$$

2.2 UV/VIS titration

3.0 ml aliquots of a 162 μM solution of **1** were pH adjusted using 0.1 M HClO_4 and 0.1 M $\text{N}(\text{CH}_3)_4\text{OH}$. The UV/VIS spectra were collected on a Cary Bio 300 and corrected for dilution (see fig. S3). No background salt was used.

A pK_a , $3.4 \pm 0.0(2)$, was determined by fitting the absorbance to $Ab_{s_{obs,400nm}} = (1 - x_A)Ab_{s_{HA,400nm}} + x_A Ab_{s_{A,400nm}}$ (*c.f.* eq. S9). See figure 2B.

3 ^{17}O NMR spectroscopy

3.1 Data acquisition

Samples for rate measurements contained 0.5 mM $[\text{Mn}(\text{H}_2\text{O})_6][\text{NO}_3]_2$ or 1.94 mM **1**, and the pH was set using HClO_4 or NaOH . All solutions contained 0.1 M NaClO_4 , used isotopically normal water unless otherwise

specified, and were spiked with 5 μl 20%- ^{17}O enriched water per 500 μl . Spectra were collected on a Bruker DRX 400 instrument (9.4 T, ^{17}O 54.26 MHz) using a $\pi/2$ pulse width (11.25 μs), 256 repetitions and with a 0.5 s recycle delay. The temperature was set to 270–336 K, and was recorded using a T-type thermocouple inserted into a dummy sample. The instrument was shimmed using an external 0.1 M NaClO_4 D_2O sample. Reference samples were made up using 0.1 M NaClO_4 and the pH was adjusted to match the sample. Line widths were fitted using a Lorentzian function. The results are tabulated in tables S1-S8.

Table S1: ^{17}O NMR line widths of the bulk water signal in the presence of 1.94 mM **1** in 0.1 M NaClO_4 at pH 3.2.

T (K)	Reference width (Hz)	Sample width (Hz)
274.15	92.37 \pm 1.32	239.37 \pm 1.16
276.40	85.49 \pm 1.12	248.56 \pm 1.10
277.85	77.08 \pm 0.99	249.27 \pm 1.18
281.10	75.45 \pm 0.99	262.17 \pm 1.24
285.90	61.38 \pm 0.76	278.12 \pm 1.5
289.55	57.16 \pm 0.65	290.03 \pm 1.76
293.15	50.03 \pm 0.58	306.95 \pm 1.81
298.95	43.57 \pm 0.47	326.66 \pm 2.07
309.75	39.52 \pm 0.42	326.66 \pm 2.11
315.10	31.06 \pm 0.31	310.90 \pm 2.02

Table S2: ^{17}O NMR line widths of the bulk water signal in the presence of 1.94 mM **1** in 0.1 M NaClO_4 at pH 4.0.

T (K)	Reference width (Hz)	Sample width (Hz)
274.15	87.35 \pm 1.26	135.23 \pm 0.48
276.40	86.57 \pm 1.15	133.10 \pm 0.41
277.85	81.33 \pm 1.03	133.23 \pm 0.45
281.10	73.6 \pm 0.91	129.08 \pm 0.49
285.90	63.05 \pm 0.79	128.43 \pm 0.46
289.55	56.05 \pm 0.68	130.56 \pm 0.47
293.15	51.47 \pm 0.6	135.38 \pm 0.50
298.95	44.27 \pm 0.50	138.23 \pm 0.54
309.75	40.07 \pm 0.43	140.87 \pm 0.59
304.30	35.72 \pm 0.38	141.44 \pm 0.68
315.10	31.44 \pm 0.31	137.71 \pm 0.66
319.35	29.09 \pm 0.29	138.35 \pm 0.62
324.10	26.28 \pm 0.25	134.4 \pm 0.65

3.2 Data processing

$$\frac{1}{T_{2p}} = \pi(\Delta\nu_{obs} - \Delta\nu_{solvent}) \quad (\text{S11})$$

$$= P_m k_m \left[\frac{\frac{1}{(T_{2m})^2} + \frac{k_m}{T_{2m}} + \Delta\omega_m^2}{\left(\frac{1}{T_{2m}} + k_m\right)^2 + \Delta\omega_m^2} \right] \quad (\text{S12})$$

Table S3: ^{17}O NMR line widths of the bulk water signal in the presence of 1.94 mM **1** in 0.1 M NaClO_4 at pH 5.0.

T (K)	Reference width (Hz)	Sample width (Hz)
275.40	93.5±0.99	112.35±0.44
281.25	76.04±0.73	101.54±0.3
287.20	63.04±0.59	98.02±0.28
293.15	55.33±0.45	95.82±0.27
298.15	46.95±0.37	96.06±0.27
303.30	45.31±0.36	100.28±0.28
310.80	38.27±0.28	98.16±0.28
320.55	31.80±0.24	95.31±0.30
332.95	25.78±0.19	94.81±0.31

Table S4: ^{17}O NMR line widths of the bulk water signal in the presence of 1.94 mM **1** in 0.1 M NaClO_4 at pH 6.0.

T (K)	Reference width (Hz)	Sample width (Hz)
284.05	95.43±1.01	109.83±0.28
287.02	86.68±0.92	103.02±0.36
293.15	75.19±0.74	99.08±0.29
298.15	64.14±0.64	97.31±0.29
303.30	57.13±0.52	101.42±0.27
310.80	47.36±0.41	100.2±0.29
320.55	39.65±0.33	99.15±0.28
332.95	32.31±0.28	100.16±0.32

Exchange rates were determined using the formalism developed by Swift and Connick.[5] Briefly, Swift and Connick described the complex relationship between the line-width of the bulk water ^{17}O NMR signal in the presence of paramagnetic aquo-complexes, and the ratio of bound to free water (P_m), the rate of exchange (k_m), the transverse relaxation rate of the oxygen in the bound water (T_{2m}), and the difference in resonance frequency between the oxygen in the bulk water and the bound ligand $\Delta\omega_m$ (eq. S12).[5, 6] Crucially, they recognised that in temperature regions where the relaxation is rapid and controlled by the change in precessional frequency ($\Delta\omega_m \gg \frac{1}{T_{2m}}$) or where T_{2m} relaxation is fast and $\frac{1}{T_{2p}}$ is dominated by exchange ($\frac{1}{T_{2m}} \gg \Delta\omega_m$), then equation S12 is reduced to $\frac{1}{T_{2p}} \approx P_m k_m$ (see eq. S13, with k_m dependent on temperature according to the Eyring-Polanyi equation).[7] However, it is common to attempt to fit the full temperature region, but this requires that a number of other variables are known, such as the paramagnetic shift ω_m , the scalar coupling constant $\frac{A}{h}$, and the electronic longitudinal relaxation, T_{1e} , which in turn are temperature dependent and relying on other factors. For most compounds these variables aren't known, and their values are determined by curve fitting which then becomes an additional potential source of error. Because all rate data in a Swift-Connick type experiment are derived, the results must thus be treated critically.

$$\frac{1}{T_{2p}} \approx P_m k_m \quad (\text{S13})$$

In the current case, for species with long T_{1e} , such as manganese(II), $\Delta\omega_m$ is very small, and eq. S15 can be derived,[5] where $B = \frac{2^2\pi^2}{3}S(S+1)$ and $S=5/2$. [6] In cases where there's a substantial shift in the bulk signal position with temperature this can be used to determine $\frac{A}{h}$ independently of T_{1e} , and T_{1e} can be

Table S5: ^{17}O NMR line widths of the bulk water signal in the presence of 0.50 mM $[\text{Mn}(\text{OH}_2)_6]^{2+}$ in 0.1 M NaClO_4 at pH 3.2.

T (K)	Reference width (Hz)	Sample width (Hz)
276.70	89.86±1.22	183.42±0.75
280.40	71.35±1.01	182.85±0.97
284.20	66.11±0.86	205.77±1.00
289.80	58.31±0.75	233.52±1.24
293.15	51.78±0.61	260.94±1.50
300.15	43.23±0.47	307.74±2.00
310.45	35.48±0.39	351.25±2.53
322.30	29.07±0.30	379.88±3.01
336.10	24.21±0.24	349.86±2.83

Table S6: ^{17}O NMR line widths of the bulk water signal in the presence of 0.50 mM $[\text{Mn}(\text{OH}_2)_6]^{2+}$ in 0.1 M NaClO_4 at pH 4.0.

T (K)	Reference width (Hz)	Sample width (Hz)
276.70	88.81±1.23	180.72±0.76
280.40	73.10±1.03	181.90±1.03
284.20	66.96±0.83	205.17±1.04
289.80	57.10±0.70	227.72±1.30
293.15	51.74±0.59	259.51±1.52
300.15	43.70±0.50	296.34±2.03
310.45	35.82±0.37	369.71±2.46
322.30	28.73±0.28	374.89±2.98
336.10	24.21±0.28	332.50±2.78

determined either via fitting or by noting that the largest value for $\frac{1}{T_{2p}}$ is dependent only on $\frac{A}{h}$ and T_{1e} . [8]. That is, however, not the case for **1**, where there is no observable bulk water signal shift with temperature.

$$\frac{1}{T_{2p}} = \frac{P_m}{\frac{1}{k_m} + T_{2m}} \quad (\text{S14})$$

$$= \frac{P_m}{\frac{1}{k_m} + \frac{1}{B\left(\frac{A}{h}\right)^2} \left(\frac{1}{T_{1e}} + k_m \right)} \quad (\text{S15})$$

Note that for very long T_{1e} ($T_{1e} > 10^{-6}$), $\frac{1}{B\left(\frac{A}{h}\right)^2 T_{1e}} \approx 0$, decoupling the equation from T_{1e} , which adds complications in fitting using this model as the sensitivity to T_{1e} varies with the value.

For $\text{Mn}(\text{H}_2\text{O})_6^{2+}$ we used $T_{1e} 1.25 \cdot 10^{-8}\text{s}$, as reported by Ducommun et al. [9] However, for **1** T_{1e} is not known, and so it was attempted to determine it through fitting by varying T_{1e} and optimising ΔH^\ddagger , ΔS^\ddagger and $\frac{A}{h}$ (see figures S4-S7). Only for pH 4.0 was a minimum for the RMS value found, at $T_{1e} 5.25 \cdot 10^{-8}\text{s}$.

Table S7: ^{17}O NMR line widths of the bulk water signal in the presence of 0.50 mM $[\text{Mn}(\text{OH}_2)_6]^{2+}$ in 0.1 M NaClO_4 at pH 5.0.

T (K)	Reference width (Hz)	Sample width (Hz)
276.70	86.91±1.17	186.70±0.70
280.40	71.76±1.14	190.92±0.96
284.20	68.17±0.87	209.00±1.02
289.80	60.65±0.74	234.12±1.25
293.15	52.25±0.61	266.67±1.54
300.15	44.78±0.49	304.89±1.89
310.45	36.84±0.39	363.54±2.41
322.30	29.16±0.29	374.53±2.93
336.10	24.19±0.23	352.31±2.59

Table S8: ^{17}O NMR line widths of the bulk water signal in the presence of 0.50 mM $[\text{Mn}(\text{OH}_2)_6]^{2+}$ in 0.1 M NaClO_4 at pH 6.0.

T (K)	Reference width (Hz)	Sample width (Hz)
276.70	97.82±1.44	213.08±0.57
280.40	80.88±1.16	215.38±0.72
284.20	74.14±0.95	213.24±0.77
289.80	64.05±0.84	250.46±0.85
293.15	59.85±0.72	285.25±1.23
300.15	48.80±0.57	315.31±1.38
310.45	40.32±0.45	368.25±1.74
322.30	32.67±0.34	380.64±2.08
336.10	26.73±0.28	352.22±1.78

3.3 Calculation of rate using difference in line-width with and without paramagnetic ion

$$\pi(\Delta\nu_{obs.} - \Delta\nu_{solvent}) = \frac{P_m}{\frac{1}{k_m} + \frac{1}{B(\frac{A}{h})^2} \left(\frac{1}{T_{1e}} + k_m \right)} \Leftrightarrow \quad (\text{S16})$$

$$\frac{P_m}{\pi(\Delta\nu_{obs.} - \Delta\nu_{solvent})} = \frac{1}{k_m} + \frac{1}{B(\frac{A}{h})^2} \left(\frac{1}{T_{1e}} + k_m \right)$$

$$km = - \frac{\left(\sqrt{(T_{1e}^2(\frac{A}{h})^4 B^2 X^2 - 2T_{1e}(\frac{A}{h})^2 BX - 4T_{1e}^2(\frac{A}{h})^2 B + 1)} - T_{1e}(\frac{A}{h})^2 BX + 1 \right)}{2T_{1e}} \quad (\text{S17})$$

where $X = \frac{P_m}{\pi(\Delta\nu_{obs.} - \Delta\nu_{solvent})}$

3.4 Error propagation

The rates are affected by variability in two parameters: $\frac{A}{h}$ and $\Delta\nu$ (or X). Assuming that they are uncorrelated, the uncertainty in rates is given by:

$$\delta km = \sqrt{\left(\frac{\partial km}{\partial(\frac{A}{h})}\right)^2 \cdot \left(\delta\left(\frac{A}{h}\right)\right)^2 + \left(\frac{\partial km}{\partial X}\right)^2 \cdot (\delta X)^2} \quad (\text{S18})$$

where, δ represents uncertainties. After taking partial derivatives,

$$\frac{\partial km}{\partial(\frac{A}{h})} = \frac{T_{1e}(\frac{A}{h})^3 B^2 X^2 - 2T_{1e}(\frac{A}{h})B - (\frac{A}{h})BX}{\sqrt{(T_{1e}^2(\frac{A}{h})^4 B^2 X^2 - 2T_{1e}(\frac{A}{h})^2 BX - 4T_{1e}^2(\frac{A}{h})^2 B + 1)}} - \frac{B(\frac{A}{h})X}{2} \quad (\text{S19})$$

$$\frac{\partial km}{\partial X} = \frac{T_{1e}(\frac{A}{h})^4 B^2 X - (\frac{A}{h})^2 B}{2\sqrt{(T_{1e}^2(\frac{A}{h})^4 B^2 X^2 - 2T_{1e}(\frac{A}{h})^2 BX - 4T_{1e}^2(\frac{A}{h})^2 B + 1)}} - \frac{(\frac{A}{h})^2 B}{2} \quad (\text{S20})$$

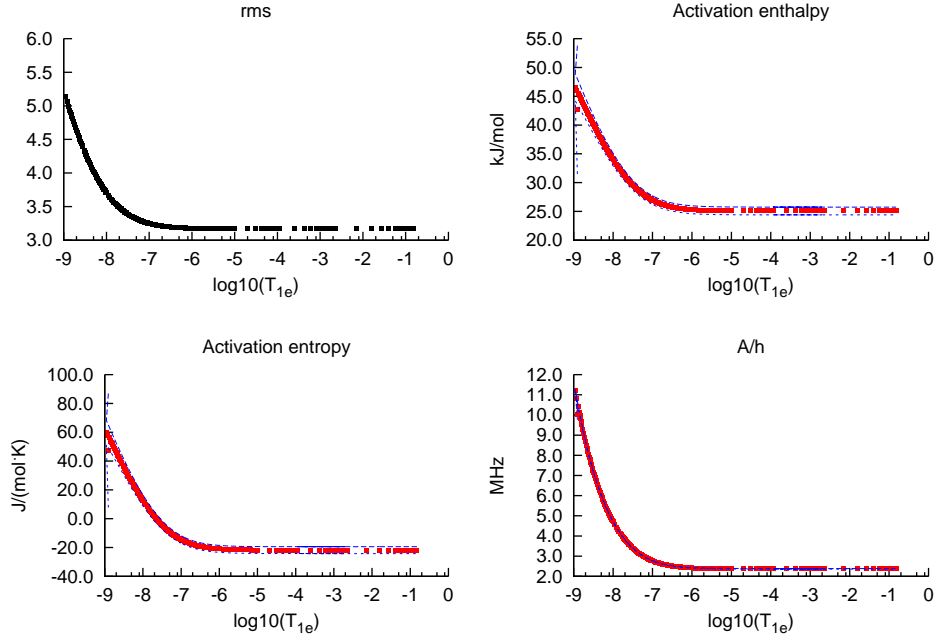


Figure S4: Fitting variables for the data of **1** at pH 3.2. Top left: Root of mean square of residual of $\frac{1}{T_{2p}}$ as a function of T_{1e} . Top right: ΔH^\ddagger as a function of T_{1e} . Bottom left: ΔS^\ddagger as a function of T_{1e} . Bottom right: $\frac{A}{h}$ as a function of T_{1e} . The dotted blue lines indicate the \pm error for each variable.

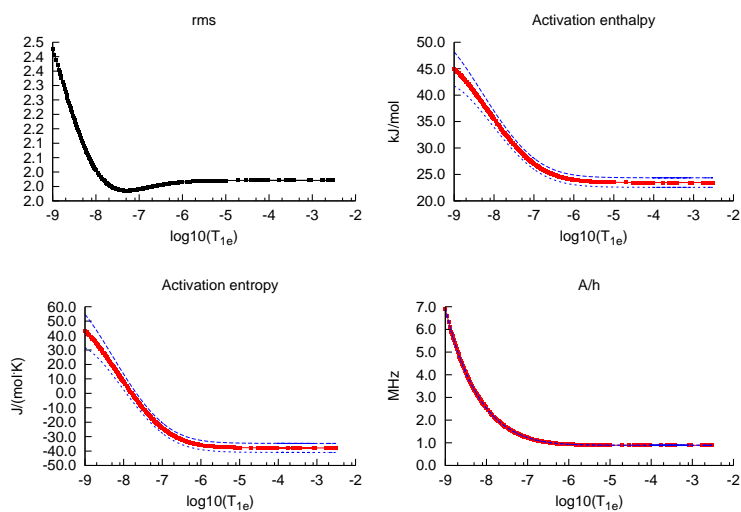


Figure S5: Fitting variables for the data of **1** at pH 4.0. Top left: Root of mean square of residual of $\frac{1}{T_{2p}}$ as a function of T_{1e} . The minimum is at $T_{1e} = 5.25 \cdot 10^{-8}$ s. Top right: ΔH^\ddagger as a function of T_{1e} . Bottom left: ΔS^\ddagger as a function of T_{1e} . Bottom right: $\frac{A}{h}$ as a function of T_{1e} . The dotted blue lines indicate the \pm error for each variable.

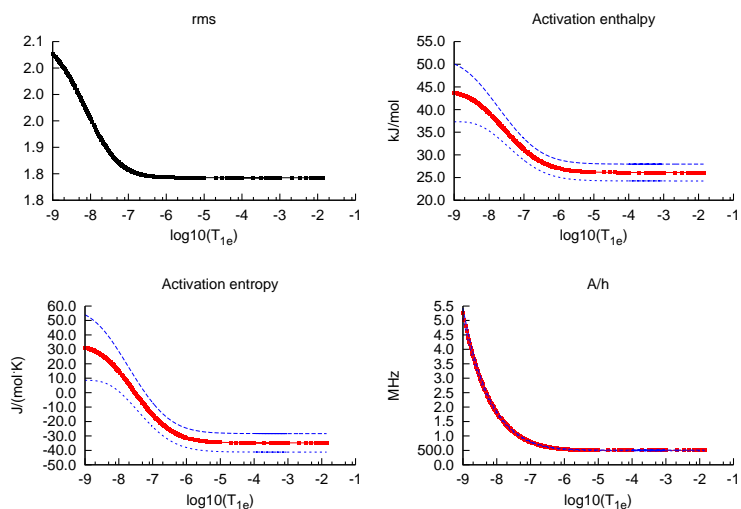


Figure S6: Fitting variables for the data of **1** at pH 5.0. Top left: Root of mean square of residual of $\frac{1}{T_{2p}}$ as a function of T_{1e} . Top right: ΔH^\ddagger as a function of T_{1e} . Bottom left: ΔS^\ddagger as a function of T_{1e} . Bottom right: $\frac{A}{h}$ as a function of T_{1e} . The dotted blue lines indicate the \pm error for each variable.

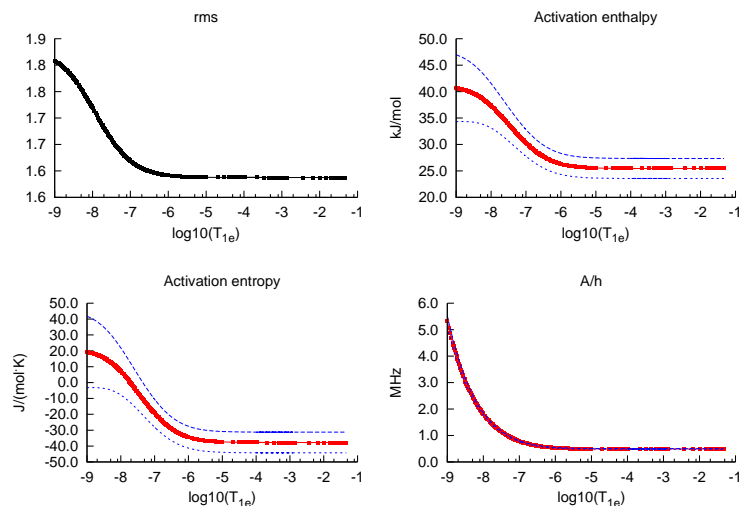


Figure S7: Fitting variables for the data of **1** at pH 6.0. Top left: Root of mean square of residual of $\frac{1}{T_{2p}}$ as a function of T_{1e} . Top right: ΔH^\ddagger as a function of T_{1e} . Bottom left: ΔS^\ddagger as a function of T_{1e} . Bottom right: $\frac{A}{h}$ as a function of T_{1e} . The dotted blue lines indicate the \pm error for each variable.

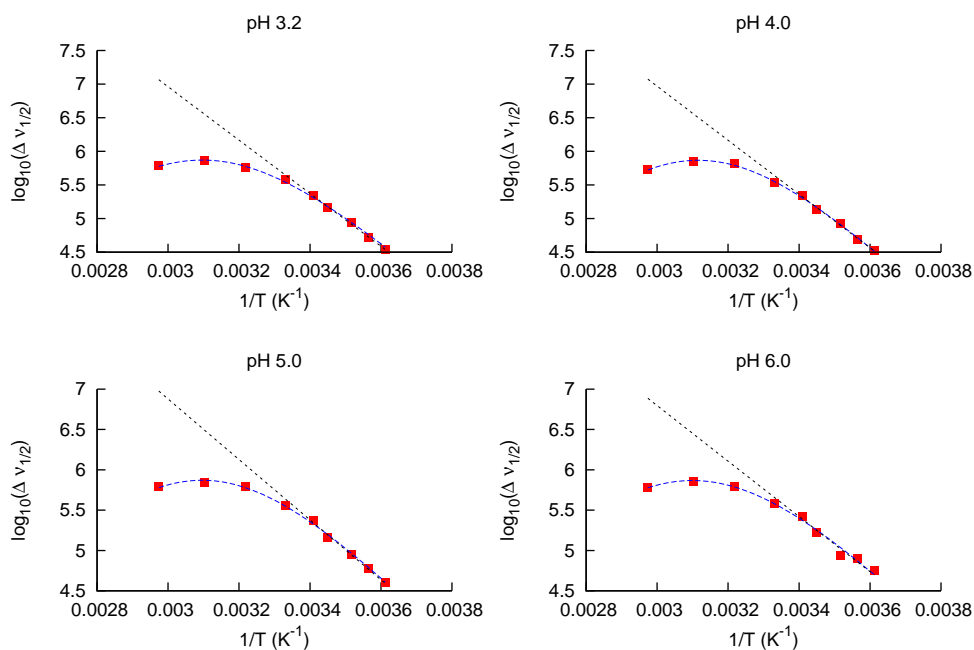


Figure S8: VT NMR data for $[\text{Mn}(\text{H}_2\text{O})_6]^{2+}$ at different pH. Blue dotted line shows best fit using eq. S15. Black dotted line shows best fit using equation S13. Top left: pH 3.2. Top right: pH 4.0. Bottom left: pH 5.0. Bottom right: pH 6.0.

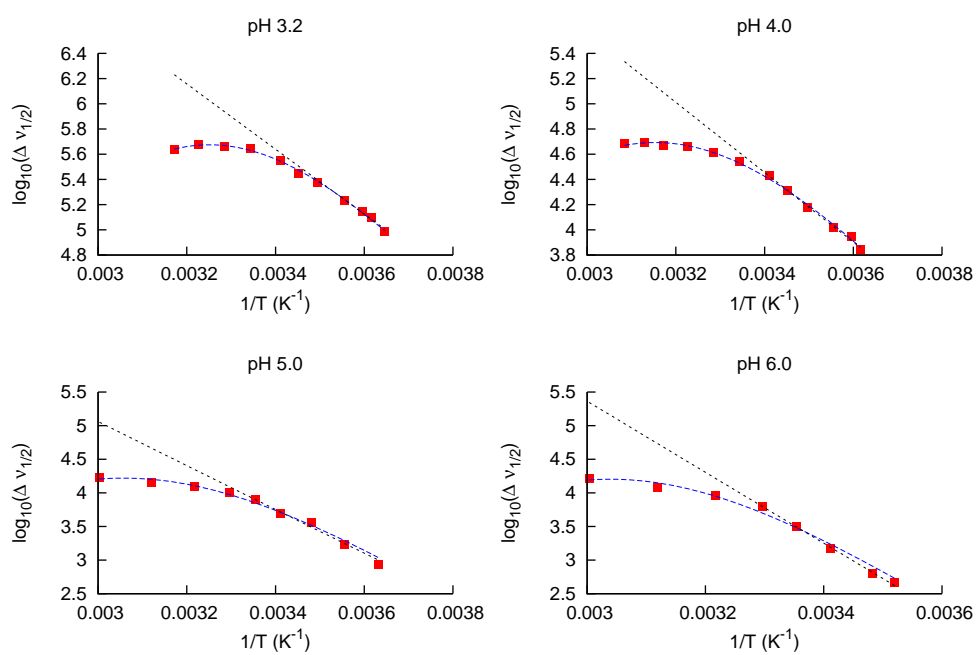


Figure S9: VT NMR data for **1** at different pH. Blue dotted line shows best fit using eq. S15. Black dotted line shows best fit using equation S13. Top left: pH 3.2. Top right: pH 4.0. Bottom left: pH 5.0. Bottom right: pH 6.0.

References

- [1] R. Contant, *Inorg. Synth.* **1990**, *27*, 104–108.
- [2] C. J. Gómez-García, J. J. Borrás-Almenar, E. Coronado, L. Ouahab, *Inorg. Chem.* **1994**, *33*, 4016–4022.
- [3] L. Ruhmann, C. Costa-Coquelard, J. Canny, R. Thouvenot, *Eur. J. Inorg. Chem.* **2002**, *4*, 975–986.
- [4] C. A. Ohlin, S. J. Harley, J. G. McAlpin, R. K. Hockin, B. Q. Mercado, R. L. Johnson, E. M. Villa, M. K. Fidler, M. M. Olmstead, L. Spiccia, R. D. Britt, W. H. Casey, *Chem. Eur. J.* **2011**, *17*, 4408–4417.
- [5] T. J. Swift, R. E. Connick, *J. Chem. Phys.* **1962**, *37*, 307–320.
- [6] T. J. Swift, R. E. Connick, *J. Chem. Phys.* **1964**, *41*, 2553.
- [7] S. J. Harley, C. A. Ohlin, W. H. Casey, *Geochim. Cosmochim. Acta* **2011**, *75*, 3711–3725.
- [8] M. S. Zetter, M. W. Grant, E. J. Wood, H. W. Dodgen, J. P. Hunt, *Inorg. Chem.* **1972**, *11*, 2701–2706.
- [9] Y. Ducommun, K. E. Newman, A. E. Merbach, *Inorg. Chem.* **1980**, *19*, 3696–3703.